Improving the Oral Bioavailability of the Iron Chelator HBED by Breaking the Symmetry of the Intramolecular H-Bond Network†

Bernard Faller,* Carsten Spanka, Thomas Sergejew, and Vincenzo Tschinke

Research Department, Novartis Pharma AG, WKL-122.P.33, CH-4002 Basel, Switzerland

Received May 25, 1999

Physicochemical analysis and Monte Carlo simulations were used to identify structural features which prevent oral absorption of HBED, a potent iron chelator. In water the dominant conformations of HBED involve the hydrophobic collapse of the two aromatic rings. These conformations are favored in polar media because they expose the polar phenolic hydroxy groups to the solvent and partially shield the nonpolar aromatic rings. In a less polar solvent such as chloroform, a symmetrical H-bond network between the carboxylates and the amines dominates the conformational space. This leads to the exposure of the phenolic hydroxy groups to the solvent, which is unfavorable for solvation. The low solubility of HBED in nonpolar solvents was confirmed experimentally by determination of the partition coefficients in octanol, chloroform, and cyclohexane and may explain the poor membrane permeability of this compound. The high conformational stability which disfavors partitioning into phospholipids is mainly due to the symmetrical H-bond network. Potentiometric titrations of a monoester of HBED in MeOH/water indicate that the protonation sequence was changed compared to that of the parent compound, suggesting that the symmetrical H-bond network was disrupted. Conformational analysis in chloroform confirmed that, in contrast to HBED, no symmetric interaction between the carboxylate and the nitrogen amines is possible in the half-ester and a variety of conformations which allow partial shielding of the polar phenolic OH groups are energetically possible. This theoretical model predicting a better solubility of the half-esters in nonpolar solvents was supported by the large increase in the partition coefficients in octanol, chloroform, and cyclohexane measured experimentally. The high absorbability predicted by physicochemical and computer simulation methods was corroborated by in vivo experiments in marmoset monkeys where the monoethyl ester derivative of HBED was well-absorbed orally while the parent compound was nearly ineffective in the same model.

Introduction

Desferal (desferrioxamine B) has been used for the treatment of iron overload for over 30 years[1] and remains the only drug generally available for this purpose. However, despite its proven efficacy Desferal suffers from its impractical mode of application due to its short plasma half-life and poor oral bioavailability. The poor compliance to the drug of many patients, especially children, has underlined the necessity to develop alternative chelators which are orally active and safe.[2,3] HBED is a potent, hexadentate ligand which was first synthesized over 30 years ago.[4] It strongly binds ferric iron with an overall formation constant (log K_{ML}) of 40, 9 log units higher than that of desferrioxamine B and several orders of magnitude higher than that of serum transferrin, making this molecule a very potent ligand for the chelation of ferric iron in vivo. Encouraging results initially came from pharmacological studies in rodents where the compound turned out to be effective and safe.[5] However, the good oral bioavailability originally observed in rats could not be reproduced in a primate model[6] (*Cebus* monkey), a more relevant animal model for human iron metabolism and drug absorption. This disappointing result observed in primates was confirmed by a phase I clinical trial[7,8] with β-thalassemia patients where oral HBED was almost ineffective compared to sc DFO, due to poor absorption of the drug. Because of the otherwise attractive properties of HBED, many attempts to improve its oral bioavailability have been undertaken. Pitt et al.[9] made a series of HBED esters by reacting the charged carboxylate groups with simple alcohols. The dimethyl ester derivative was extensively studied and was found very potent in rodents but, again, failed to be effective in *Cebus* monkeys[6] apparently because the *Cebus* is not able to hydrolyze HBED esters once taken up from the gut.

This manuscript reports on the physicochemical properties of new HBED derivatives, which do not necessitate enzymatic cleavage and which retain oral activity in primates.

Results

Chemistry. HBED monoalkyl esters **3** were prepared by partial hydrolysis of the dialkyl esters **2** with 1 equiv of sodium hydroxide in the corresponding alcohol. The

† Abbreviations: HBED (**1**), *N*,*N*′-bis(2-hydroxybenzyl)ethylenediamine-*N*,*N*′-diacetic acid hydrochloride dihydrate; dm-HBED (**2a**), dimethyl *N*,*N*′-bis(2-hydroxybenzyl)ethylenediamine-*N*,*N*′-diacetate; de-HBED (**2b**), diethyl *N*,*N*′-bis(2-hydroxybenzyl)ethylenediamine-*N*,*N*′-diacetate; mm-HBED (**3a**), sodium *N*,*N*′-bis(2-hydroxybenzyl)-ethylenediamine-*N*-methoxycarbonylmethyl-*N*′-acetate; me-HBED (**3b**), sodium *N*,*N*′-bis(2-hydroxybenzyl)ethylenediamine-*N*-ethoxycarbonylmethyl-*N*′-acetate; EDDA, ethylenediaminediacetic acid; EHPG, *N*,*N*′-ethylenebis(*o*-hydroxyphenyl)glycine; po, per os; sc, subcutaneous.

* To whom correspondence should be addressed. Tel: +41 61 696 5406. Fax: +41 61 696 8663. E-mail: bernard.faller@pharma.novartis.com.

10.1021/jm990261n CCC: $19.00
Published on Web 03/28/2000

Scheme 1[a]

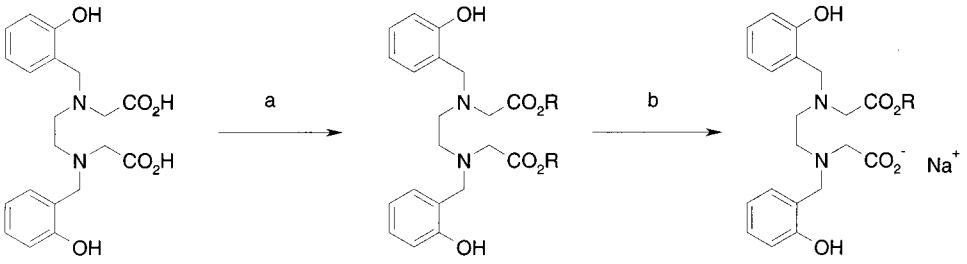

1 **2a** R = Me, 94% **2b** R = Et, 79% **3a** R = Me, 51% **3b** R = Et, 86%

[a] Reagents and conditions: (a) 10% HCl(g) in ROH, 50 °C, 18 h; (b) 1.0 equiv 2 M NaOH, ROH, 40 °C, 18 h.

Scheme 2[a]

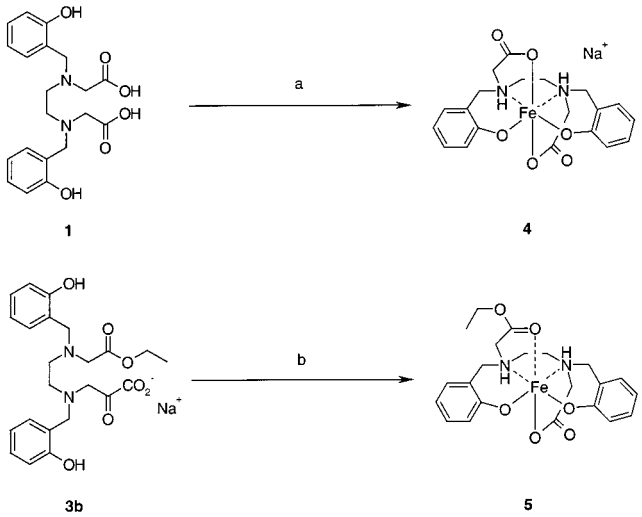

1 **4** **3b** **5**

[a] Reagents and conditions: (a) 1 equiv $FeCl_3 \cdot 6H_2O$, 2 M HCl, 30 °C, 30 min, then 4 M NaOH, pH 10, 0 °C, 1 h; (b) 1 equiv $FeCl_3 \cdot 6H_2O$, EtOH, 0 °C, 30 min, then 1 M NaOH pH 3, 2 h, rt.

desired compounds precipitate directly from the reaction mixture and were isolated in the form of their monosodium salts which are stable, nonhygroscopic solids. The required HBED dialkyl esters **2**[9] were synthesized by hydrogen chloride-catalyzed esterification of HBED (**1**) with alcohols.The iron complexes **4** and **5** were prepared by treatment of the free ligands **1** and **3b** with 1 equiv of iron(III) chloride hexahydrate followed by neutralization with sodium hydroxide.

Ionization Constants. HBED (**1**), mm-HBED (**3a**), and me-HBED (**3b**) are soluble in water within a large pH range which allows direct measurement of the majority of their aqueous ionization constants. The water solubility of the diesters (**2a** and **2b**) is so small that direct potentiometric titration in water is not possible. In these cases, titrations were performed in the presence of different amounts of cosolvent (MeOH and EtOH, respectively) and the aqueous pK_a's were extrapolated using the method of Yasuda and Shedlowsky.[10,11] The low pK_a's were determined by spectrophotometric titration because of the poor performance of the pH electrode under very acidic conditions (pH < 2).

Titrations in mixed-solvent media were also used to identify microspecies present in solution. Although pH metric titration cannot identify protonation sites in the molecule, the variation of the ionization constants with the dielectric constant can be used to distinguish between acid and base functions.[21] In the presence of a cosolvent of dielectric constant lower than water, equilibria with overall decreased charges are favored. Thus, in the case of a weak acid the pK_a will increase as the dielectric constant of the titration medium is decreased. Results are presented in Table 1.

With HBED, the aqueous pK_a's determined by potentiometric titration compare very well with the values reported earlier by L'Eplattenier[4] (Table 2). The analysis of the slope of the pK_a vs % cosolvent plot indicates that pK_{a3} and pK_{a4} correspond to the association of protons with the basic amino groups. The same conclusion was drawn by L'Eplattenier using another method (comparison of the pK_a's of HBED with related compounds, EDDA and EHPG). The sequence of protonation of HBED involves the two phenols first, followed by the two amines and the two carboxylates. This sequence of events strongly suggests the existence of zwitterions in solution (Table 3).

With the two diesters 2a and 2b, the aqueous pK_a's were obtained using a cosolvent approach. The presence of the cosolvent (i) maintains the compound in solution allowing potentiometric titration to be performed and (ii) protects the esters from being hydrolyzed at alkaline pH by shifting the equilibrium toward diester formation. For this reason, MeOH was used with **2a** and EtOH with **2b**. Comparison of the protonation constants with those of HBED showed little difference for the phenols, whereas the amino group pK_a's are significantly lower in the diesters than in HBED itself.

With the two monoesters 3a and 3b, the aqueous pK_a's could be determined directly by potentiometric titration in 0.15 M KCl. Even at alkaline pH no ester cleavage was observed during the titration indicating that the ester bonds are relatively stable. Determination of the pK_a's in media with different dielectric constants was also performed to identify microspecies. This analysis shows a different sequence of protonation compared to HBED, with an inversion between the amino group and the carboxylates (Table 3). This is the consequence of the disrupted symmetry of the molecule as compared to the diesters or to HBED itself.

Partition Coefficients. Calculated log $P_{o/w}$: Theoretical ocanol/water partition coefficients were generated using two different software packages. The ACD log *P* (from Advanced Chemistry Development Inc., Canada) uses a structure−fragment approach. The second program was developped in-house and calculates partition coefficients using an atom-based approach following the method proposed by Wakita et al.[12] Data are summarized in Table 4a.

Table 1. Ionization Constants for HBED and Its Methyl and Ethyl Ester Derivatives[a]

compd	cosolvent	dielectric constant	pK_{a1}	pK_{a2}	pK_{a3}	pK_{a4}	pK_{a5}	pK_{a6}
1	none	78	**12.90 (0.80)**	**11.10 (0.03)**	**8.34 (0.02)**	**4.61 (0.01)**	nd	nd
	YS		nd	nd	8.36	4.58	**1.62**	**0.92**
	MeOH	62	nd	nd	8.36 (0.01)	4.58 (0.02)	2.25 (0.05)	1.05 (0.02)
	MeOH	56	nd	12.53 (0.10)	8.36 (0.01)	4.57 (0.01)	2.34 (0.02)	1.11 (0.02)
	MeOH	49	nd	nd	8.37 (0.01)	4.71 (0.01)	2.72 (0.02)	1.18 (0.02)
3a	none	78	**12.05 (0.05)**	**10.93 (0.01)**	**7.67 (0.01)**	**2.61 (0.01)**	nd	
	YS		nd	11.50	7.68	2.49	**1.30**	
	MeOH	62	nd	11.81 (0.02)	7.56 (0.01)	2.68 (0.01)	1.15 (0.02)	
	MeOH	56	nd	12.05 (0.02)	7.48 (0.01)	2.77 (0.01)	0.97 (0.02)	
	MeOH	49	nd	12.22 (0.02)	7.41 (0.01)	2.94 (0.01)	0.90 (0.02)	
2a	YS		**12.2**	**10.90**	**5.70**	**1.40**		
	MeOH	62	12.60 (0.15)	11.34 (0.02)	5.58 (0.01)	1.10 (0.01)		
	MeOH	56	12.91 (0.25)	11.55 (0.02)	5.46 (0.01)	0.82 (0.02)		
	MeOH	49	nd	11.87 (0.06)	5.40 (0.02)	0.69 (0.02)		
3b	none	78	**12.31 (0.30)**	**10.91 (0.05)**	**7.64 (0.03)**	**2.91 (0.03)**	**0.90 (0.04)**	
	EtOH	63	nd	11.44 (0.05)	7.50 (0.03)	2.75 (0.05)	nd	
2b	YS		**12.20***	**10.90***	**5.70**	**1.80**		
	EtOH	63	nd	nd	5.45 (0.02)	1.42 (0.25)		
	EtOH	57	nd	11.55 (0.02)	5.25 (0.01)	1.21 (0.13)		
	EtOH	52	nd	11.80 (0.02)	5.09 (0.01)	1.05 (0.25)		

[a] nd, not determined; *estimated by analogy with **2a**; YS, Yasuda−Shedlovsky extrapolation to zero cosolvent from mixed solvent titrations. The best values for the aqueous pK_a are indicated in bold. Standard deviations are indicated in parentheses.

Table 2. Comparison of the Aqueous Ionization Constants for HBED with Literature Values

pK_{a1}	pK_{a2}	pK_{a3}	pK_{a4}	pK_{a5}	pK_{a6}	remarks	ref
12.90	11.10	8.34	4.61	1.62.	0.92	0.15 M KCl	this work
12.46	11.00	8.32	4.64	nd	nd	0.1 M KNO_3	1

Table 3. Assignment of Chemical Functions to Ionization Constants[a]

compd	pK_{a1}	pK_{a2}	pK_{a3}	pK_{a4}	pK_{a5}	pK_{a6}
1	12.90	11.10	8.34	4.61	1.62	0.92
chem group	P-OH	P-OH	N	N	COOH	COOH
3a	12.05	10.93	7.67	2.61	1.30	
chem group	P-OH	P-OH	N	COOH	N	
2a	12.20	10.90	5.70	1.40		
chem group	P-OH	P-OH	N	N		
3b	12.31	10.91	7.64	2.91	0.90	
chem group	P-OH	P-OH	N	COOH	N	
2b	12.20	10.90	5.70	1.80		
chem group	P-OH	P-OH	N	N		

[a] P-OH, phenolic OH; N, nitrogen amine; COOH, carboxylate.

Experimental partition coefficients: Dual-phase titrations were used to measure the partition coefficients in octanol, chloroform, and cyclohexane. Partition coefficients reported in this work refer to macroconstants[13] which means that the values refer to overall tautomeric equilibria of the given species. Data are summarized in Table 4a.

In 1-octanol, the two diesters **2a** and **2b** are much more soluble than the three other compounds. The dm-HBED (**2a**) has a log *P* of 2.86, and the addition of two carbons further increases the log *P* to 3.35 for the diethyl ester (**2b**). In contrast to what was predicted in silico, compounds **3a** and **3b** are significantly more soluble in octanol than **1a** (0.5 and 1.15 vs 0.16, respectively).

In chloroform, the solubility of compounds **3a** and **3b** is again higher than that of **1a** but the difference between the half-esters **3a** and **3b** and free HBED (**1a**) is higher than in octanol.

In cyclohexane, only the two diesters have positive log *P* values. The partitioning of both HBED and mm-HBED (**3a**) was very small (log $P < -2$) and could not be measured. In this aprotic solvent me-HBED (**3b**) is significantly more soluble than mm-HBED (**3a**).

Table 4.

a: Partition Coefficients (in log units) in Different Solvents[a]

compd	molecular species partition	fragment-based calcd	atom-based calcd	octanol	chloroform	cyclohexane
1	$(LH4)^0$	3.4	2.2	0.16 (0.06)	<−2	<−2
3a	$(LH3)^0$	3.8	2.2	0.50 (0.05)	−0.29 (0.05)	<−2
2a	$(LH2)^0$	4.1	2.3	2.86 (0.03)	nd	2.11 (0.06)
3b	$(LH3)^0$	4.3	2.6	1.15 (0.05)	0.18 (0.03)	−1.30 (0.10)
2b	$(LH2)^0$	5.2	3.0	3.35 (0.05)	3.35 (0.05)	3.22 (0.09)

b: Hydrogen-Bonding Potentials

compd	H-bond acidity[b]	H-bond basicity[c]	H-bond total	oral activity
1	>2.2	nd	≫2.2	−
3a	0.8	>1.7	>2.5	+/−
2a	nd	nd	0.7	+
3b	1.0	1.5	2.4	+
2b	0	0.1	0.1	+/−

[a] Standard deviations are indicated in parentheses. [b] A rough estimate of H-bond acidity was obtained using $\log P_{oct} - \log P_{CHCl_3}$. [c] A rough estimate of H-bond basicity potential was obtained using $\log P_{CHCl_3} - \log P_{C_6H_{12}}$.

Conformational Analysis. Monte Carlo calculations were performed with solvent effects taken into account for water and chloroform. The protonation constants determined experimentally strongly suggest that HBED and its esters exist as zwitterions in solution. We have therefore chosen the shorter separation of the charges between the carboxylate and amine groups on the two esters (Figure 1). This study was designed to provide insight on the changes undergone by the species as they cross a water/lipid barrier. Since the species dominant in the nonpolar phase are neutral and since these species also exist in water, we restricted our analysis to the neutral species, as the most likely to cross the water/lipid barrier. Computer simulations were carried out for HBED and its monomethyl and monoethyl esters, as well as for its dimethyl ester.

Conformations in water: In water all four species (**1**−**3**) are predicted to be very flexible. The dominant conformations present a hydrophobic collapse of the two aromatic rings (Figure 2).

Conformations in chloroform: Monte Carlo simulations in a less polar solvent suggest a different behavior of HBED as opposed to its esters. HBED itself

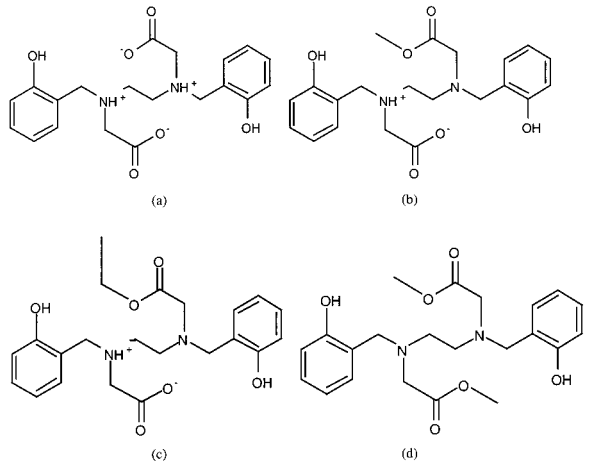

Figure 1. Two-dimensional structures with assigned protonation patterns: (a) HBED (**1**), (b) mm-HBED (**3a**), (c) me-HBED (**3b**), (d) dm-HBED (**2a**).

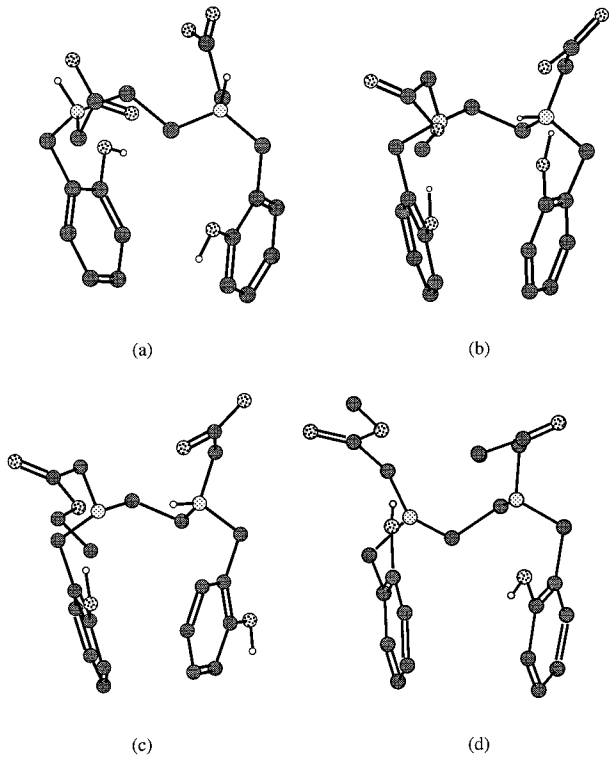

Figure 2. Low-energy conformations in water: (a) HBED (**1**), (b) me-HBED (**3a**), (c) me-HBED (**3b**), (d) dm-HBED (**2a**).

strongly prefers conformations with the two aromatic rings separated by a large distance (Figure 3a). These conformations are stabilized by an internal H-bond network between the protonated nitrogen atoms and the carboxylate groups on opposite sites of the molecule.

By contrast, both **3a** and **3b** are flexible in chloroform. They assume different conformations with shorter distances between the aromatic rings compared to HBED (Figure 3b,c). The dimethyl ester can also assume a variety of conformations with short distances between the two aromatic rings. As expected, some conformations possess a binary axis of rotation (Figure 3d). The shapes of the mono- and diesters in chloroform are less compact than in water but more compact than HBED itself in water. A critical factor influencing the shape of the molecules is the distance between the two aromatic rings (Table 5).

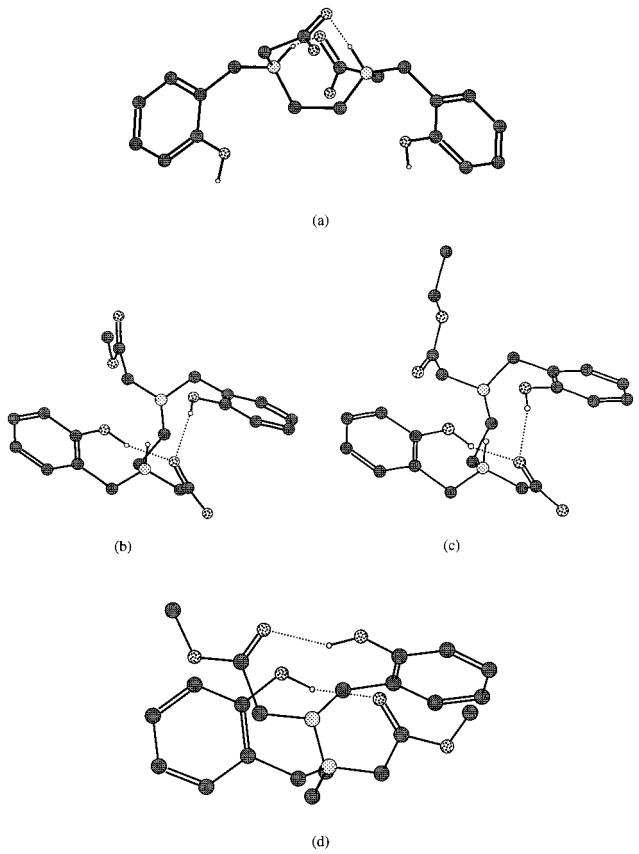

Figure 3. Low-energy conformations in chloroform: (a) HBED (**1**), (b) mm-HBED (**3a**), (c) me-HBED (**3b**), (d) dm-HBED (**2a**). In panels b and c, the thin lines indicate hydrogen bonds between the phenolic OH groups and the carboxylate group; in panel d, the thin lines indicate hydrogen bonds between the phenolic OH groups and the ester CO groups.

Table 5. Minimum and Maximum Computed Distances[a] (Å) between Aromatic Rings[b]

compd	water	chloroform
1	4.0−10.4	8.5−10.3
3a	3.8−9.6	4.4−9.5
3b	3.8−9.9	4.1−8.9
2a	3.8−9.3	4.1−9.9

[a] Obtained from the sets of Monte Carlo conformations within 4 kcal/mol of and including the lowest-energy conformation. [b] Distance between the two centroids of the aromatic rings, defined as the center of mass of the six ring carbon atoms.

Kinetic Stability of me-HBED−Fe Chelate. me-HBED−Fe (**5**) converts into HBED−Fe (**4**) in a process induced by iron. The decay of **5** into **4** can be followed easily since the two chelates can be separated by extraction with dichloromethane. **4** is much more polar than **5** and stays in the aqueous phase, while more than 99% of **5** is extracted in the organic solvent. The me-HBED−Fe chelate was dissolved in pure DMSO at an initial concentration of 5 mM. As a control, the stability of **5** in DMSO was checked. In pure DMSO the chelate was stable for at least 4 h at room temperature. At time 0, a small aliquot of the DMSO stock solution of Fe chelate was diluted into a pH 7.40 HEPES buffer. After various incubation times aliquots were taken and the Fe chelates of **3b** and **1** were separated by the addition of an equal volume of dichloromethane. The time-dependent decay of **5** and the concomitant formation of **4** were both well-described by first-order kinetics (Figure

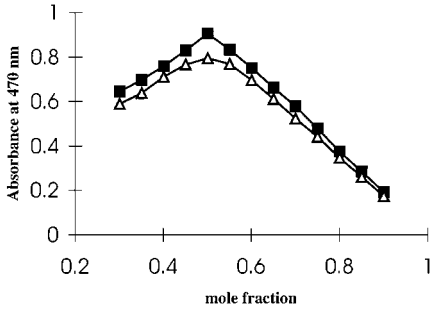

Figure 4. Job plot at pH 7.40 for HBED (**1**) and me-HBED (**3b**). The total ligand (chelator + metal ion) concentration was fixed at 0.5 mM. Filled and open symbols indicate compounds **1** and **3b,** respectively.

4). Nonlinear regression analysis gave rate constants of 0.014 and 0.015 min^{-1} for the formation of **4** (filled symbols) and the decay of **5** (open symbols), respectively.

The first-order conversion of **5** into **4** indicates that the reaction is not a process in which Fe acts as a catalyst but that one atom of Fe induces the conversion of one molecule of **3b** into one molecule of **1**. This conclusion was further substantiated in a second set of experiments where different initial concentrations of **5** (0.05, 0.10, 0.15, and 0.2 mM) were converted into **4** with similar rate constants ($k = 0.015 \pm 0.003$ min^{-1}). In conclusion, at pH 7.40 the half-time for the conversion of **5** into **4** is about 47 min ($t_{1/2} = 0.7/k$), this value being independent of the initial concentration of **5**.

Iron-Binding Stoichiometry and Stability of me-HBED−Fe. The iron-binding stoichiometry was determined at pH 7.40 using the mole ratio variation method also known as the Job plot.[28] For both **1** and **3b** the peak concentration of Fe chelate is reached at a mole ratio of 0.50 (Figure 4), indicating that the binding metal ion/ligand stoichiometry is 1:1 in both cases. A sharp peak is indicative of a high affinity of the chelator for the metal ion. Figure 4 shows that the absorbance vs mole ratio curve for **3b** is slightly more bell-shaped compared to that of **1**; a weaker binding affinity is therefore anticipated with **3b**.

The iron-binding affinity of **3b** was measured by spectrophotometric pH titration in KCl (0.15 M). Ligand and ferric iron were reacted in the presence of different H^+ concentrations (10−100 mM) in 1-mL aliquots. The spectra were recorded immediately after steady-state was reached, usually within 1−2 min. The best theoretical absorbance vs pH curve was generated using a simple model with only three species: ML and free M and L, respectively (Supporting Information). The titration was repeated with two other ligand/metal ion initial concentrations: 1.0/0.15 and 0.25/0.15 mM, respectively. Similar log K_{ML} values were found (30.6 and 30.7).

In Vivo Activity. The oral availability of the chelators was indirectly assessed by their pharmacodynamic effect (induction of iron excretion) in iron-overloaded animals. It is well-known that rodents differ from primates in drug absorption; for example HBED is orally effective in rats[6] but not in humans.[7,8] For these reasons, the compounds were evaluated in a primate model (*Callithrix jacchus*, commonly known as marmoset).

The effects of the HBED half-esters (**3a** and **3b**), compared with the parent compound (HBED), are illustrated in Table 6. Although HBED is effective when delivered by the sc route, when given orally it is only marginally active, as in humans,[7,8] while the half-esters were highly active after po application. A comparison of the iron excretion values after po and sc application (Table 6) indicates a high oral availability for **3b** in our primate model.

Table 6. Induction of Fe Excretion in Marmoset Monkeys[a]

compd	sc	po
1	1586	167
3a	nd	519
2a	968	1127
3b	1782	1412
2b	nd	739

[a] The values indicate the amount of induced Fe excretion in μg/kg of body weight after po or sc administration of 150 μmol/kg of test compound; nd, not determined.

Discussion

In water, the dominant conformations of HBED show a hydrophobic collapse of the two aromatic rings (Figure 2a). These conformations are favored in polar media because they result in the exposure of the polar groups to the solvent and partial shielding of the nonpolar hydrophobic aromatic rings.

In a less polar medium such as chloroform, HBED exhibits very different conformations. According to Monte Carlo simulations in chloroform, HBED has the tendency to assume conformations with the two aromatic rings separated by a large distance between the centroids of the aromatic rings (Table 5 and Figure 3a). These conformations are stabilized by internal hydrogen bonds between the two amines and the two carboxylates. The formation of hydrogen bonds across the two sides of a flexible molecule result in a conformation with a large distance between the two aromatic rings which also shields the polar groups from the solvent. Our conformational analysis predicts little conformational variation in a nonpolar solvent mainly because any conformational change disrupting the symmetrical H-bond network between the carboxylates and the nitrogen amines is strongly penalized energetically. For the same reason, the phenolic OH groups are not engaged in hydrogen bonds and remain exposed to the solvent. The exposure of these polar groups to the solvent results in a very low solubility of HBED in nonpolar solvents, as confirmed experimentally by the determination of the partition coefficients in chloroform/water and cyclohexane/water (both less than −2 in log units).

With the monomethyl (**3a**) and monoethyl (**3b**) esters, several opportunities to form internal hydrogen bonds are possible among the polar groups. In low polarity media such as chloroform these interactions result in a high number of conformations which allow partial shielding of the polar groups from the solvent. In contrast to HBED no symmetric interaction between the carboxylates and the nitrogen amines is possible. In addition, the polar phenolic OH groups participate in the H-bond network with other polar groups, particularly with the charged carboxylate (see Figure 3b,c and Table 6). As a result, a variety of conformations with intermediate distances between the aromatic rings are observed. The partial shielding through internal hydrogen bonds of all polar groups including the phenolic

OH's should contribute to an increased solubility of the monoesters (**3**) in nonpolar solvents. This theoretical model is supported by the experimental data showing a large increase in solubility of the monoesters in chloroform and cyclohexane (see Table 4).

Computer simulations with **2a** in chloroform gave results similar to those obtained with **3a** and **3b**, the polar phenolic OH groups being effectively shielded from the solvent by intramolecular hydrogen bonds between the tertiary amine and the ester groups.

In the second part of the discussion we want to show which physicochemical parameters are responsible for the different behavior of the monoesters compared to HBED (**1)** with respect to their oral bioavailability in marmoset monkeys. Lipophilicity and hydrogen bonds are known to be important parameters influencing membrane permeability and thus oral absorption.[14,15]

The lipophilicity of molecules is usually estimated via determination of their octanol/water partition coefficient. On the basis of calculated octanol/water partition coefficients, one did not expect major absorption differences between **1a** and compounds **3a** and **3b** as their values differ by less than 1 log unit with both programs used. When one switches to experimental octanol/water partition coefficients where the conformational aspect should be better modeled, the difference between the values of **1a** and **3b** is about 1 log unit. Strong differences between the free HBED (**1a**) and the half-esters (**3a** and **3b**) were only observed in chloroform and cyclohexane. Therefore octanol was less predictive of different po activities than chloroform or cyclohexane, presumably because of its inadequate H-bond acidity component.[16]

One way to estimate the hydrogen-bonding capability of a molecule experimentally is to measure the partition coefficients in solvents with different properties. In this study we used octanol (amphiprotic), chloroform (proton donor), and cyclohexane (aprotic). Total hydrogen-bonding potential and hydrogen-bonding acidity and basicity of the different compounds investigated are summarized in Table 4b. Several investigators have shown that, to cross a lipid bilayer, the compound needs to proceed through a desolvation step in order to accommodate the nonpolar environment of the inner layer of the phospholipid membranes. The ability of a compound to diffuse into a low-polarity environment can be estimated by measuring its relative solubility in an aprotic solvent like cyclohexane.

The data presented in Table 4b show that although the total hydrogen-bonding potential is very high for free HBED, esterification of one carboxylate translates into a reduction of the H-bond acidity and basicity. One can also notice a shift in ionization constants of **3a** vs **1** (increase of the carboxylate pK_a and decrease of the amine pK_a's). The decrease in hydrogen bonds is amplified in me-HBED (**3a**) with a total hydrogen-bonding potential of only 1.62. One can also observe a further increase in carboxylate pK_a and a decrease in amine pK_a values compared to **3a**. In contrast to HBED and **3a**, **3b** falls in a $\Delta\log P_{o/h}$ range where good oral absorption is expected.

The two diesters **2a** and **2b** are highly soluble in cyclohexane. However, in vivo data (Table 6) show that they are not more effective inducers of iron excretion than the monoester **3a** following oral application. Two possible explanations may account for this finding: (i) decreased oral absoption possibly due to the low water solubility which then becomes the limiting factor for absorption[17] and (ii) the diesters are not chelating agents by themselves and require enzymatic cleavage to be activated.

Conclusion

We have shown that the me-HBED (**3b**) is able to form 1:1 chelates with ferric iron and that its binding affinity is sufficiently high to compete successfully with endogenous ligands such as transferrin or citrate. In addition, the resulting iron chelate is converted into HBED−Fe in a nonenzymatic way.

Furthermore, Monte Carlo simulations could show that disrupting the symmetry of the parent compound (HBED) results in a major change in the H-bond network within the molecule. In low-polarity media (i.e. membrane phospholipid tails) the polar groups of the mono- and diesters are neutralized since they are engaged in internal hydrogen bonds. Measurement of the relative solubility of the compounds in chloroform and cylohexane gave experimental evidence in support of conformations predicted by computer simulation and allowed quantification of the H-bond networks. The partition coefficients summarized in Table 4a could be used to quantify the hydrogen-bonding capability of the different molecules. Experimental data showed that both H-bond acidity and basicity were decreased in me-HBED (**3b**) compared to mm-HBED (**3a**), the former compound falling within a range where good oral availability is expected. The data presented here do correlate with the observations made in monkeys. HBED half-esters represent an elegant way to gain oral activity over the parent compound, and it is reasonable to believe that it will be effective in humans as well, as no enzymatic cleavage is required to release the active compound.

Experimental Section

Materials. HBED **(1)** was purchased as dihydrochloride dihydrate from Strem Chemicals (Newburyport, MA). Larger quantities can be prepared according to the procedure published by L'Eplattenier et al.[4]

Methods. Synthesis. Melting points were determined on a Büchi B-540 melting point apparatus and are uncorrected. Thinlayer chromatography (TLC) was done on silica gel 60 F_{254} coated glass plates (Merck, Art. 5719), product spots were visualized by illumination with UV light (254 nm) or by staining with 0.1 M $FeCl_3$ in 1 M HCl. Flash column chromatography[18] was performed using silica gel 60 (230−400 mesh; Merck, Art. 9385). Purity of compounds was evaluated on a Kontron HPLC system equipped with a 465 autosampler, a 322 pump, and a 430A detector using a NUCLEOSIL 100-5 C_{18} analytical column (250 mm × 4.6 mm; Macherey-Nagel, Düren, FRG): linear gradient of 0.1% TFA in MeCN/0.1% TFA in H_2O from 20:80 to 100:0 over 11 min and 100:0 for 5 min; flow rate 1 mL/min, detection at 215 nm. Fast atom bombardment mass spectra (FAB) were taken on a ZAB-HF instrument (VG Analytical). Electrospray ionization mass spectra (ESI) were measured on a VG platform spectrometer (Fisons Instruments). ^{1}H NMR (300 MHz) spectra were recorded on a Varian GEMINI-300 spectrometer, samples were dissolved in either DMSO-d_6 or $CDCl_3$. Chemical shifts are reported in ppm (δ) using the residual solvent signal as reference (δ 7.26 for $CDCl_3$ and δ 2.49 for DMSO-d_6). The following abbreviations are used to describe the peak patterns observed: br = broad, s = singlet,

d = doublet, t = triplet, q = quartet, m = multiplet; quotation marks (e.g. 'd') are being used for higher-order signals. Coupling constants (*J*) are given in hertz (Hz). Elemental analyses were performed by Organische Elemente Analytik, Novartis Services AG, Switzerland.

***N,N′*-Bis(2-hydroxybenzyl)ethylenediamine-*N,N′*-diacetic Acid Hydrochloride Dihydrate, HBED (1).** The commercially available material was purified by the following method: HBED dihydrochloride dihydrate (20 g, 40.2 mmol) was dissolved in 2 M NaOH (250 mL), and insoluble matter was removed by suction filtration. The slightly turbid pink colored filtrate was acidified by careful addition of 2 M HCl (pH 1.5). The desired product precipitated in form of fine crystals. The suspension obtained was stirred for 3 h in an ice bath and then stored at 4 °C overnight. The crystals deposited were collected on a Buchner funnel, washed with ice water (3 × 100 mL), and vacuum-dried at 40 °C for 18 h to give **1** (15.95 g, 86%) as a light- and air-sensitive colorless powder: mp 136−141 °C dec; TLC R_f = 0.03 (DCM/MeOH/H_2O/AcOH 90:10:1:0.5); HPLC t_R = 7.50 min; ^{1}H NMR (300 MHz, DMSO-d_6) δ 3.21 (s, 4H, N-C**H$_2$**-C**H$_2$**-N), 3.66 (s, 4H, N-C**H$_2$**-CO_2H), 4.05 (s, 4H, N-**CH$_2$**-Ar), 6.78 ('t', 2H, *J* = 7.50, Ar**H**), 6.94 ('d', 2H, *J* = 8.25, Ar**H**), 7.12−7.30 (m, 4H, Ar**H**). Anal. ($C_{20}H_{24}N_2O_6$·HCl·2H_2O [460.92]) C, H, N, Cl^-, H_2O.

General Procedure for Acid-Catalyzed Esterification of HBED (1). The preparation of HBED dialkyl esters **2** was performed according to the procedure published by Pitt et al.[9] The yields could be significantly improved by utilization of gaseous hydrogen chloride instead of thionyl chloride: HBED (4.61 g, 10 mmol) was suspended in the selected alcohol (50 mL). Then HCl gas (approximately 5 g) was introduced in a moderate stream with cooling in an ice bath. After this the reaction mixture was heated to 50 °C for 18 h with stirring. The solvent was stripped off in vacuo, the residue was taken up in ethyl acetate (100 mL), washed (1× $NaHCO_3$, 2× H_2O, 1× brine), dried ($MgSO_4$), and evaporated in vacuo. The crude material was purified by flash chromatography (ethyl acetate/hexanes 1:4) and recrystallization.

Dimethyl *N,N′*-bis(2-hydroxybenzyl)ethylenediamine-*N,N′*-diacetate (2a): colorless prisms from hot methanol (3.91 g, 94%); mp 93−96 °C; TLC R_f = 0.26 (ethyl acetate/hexanes 1:2); HPLC t_R = 9.87 min; ^{1}H NMR (300 MHz, $CDCl_3$) δ 2.74 (s, 4H, N-C**H$_2$**-C**H$_2$**-N), 3.30 (s, 4H, N-C**H$_2$**-CO_2Me), 3.74 (s, 3H, CO_2**Me**), 3.76 (s, 4H, N-**CH$_2$**-Ar), 6.79 ('dt', 2H, *J* = 1.13, 7.36, Ar**H**), 6.84 ('dd', 2H, *J* = 0.95, 8.03, Ar**H**), 6.92 ('dd', 2H, *J* = 1.65, 7.48, Ar**H**), 7.19 ('dt', 2H, *J* = 1.71, 7.88, Ar**H**), 9.50 (br s, 2H, ArO**H**). Anal. ($C_{22}H_{28}N_2O_6$ [416.48]) C, H, N.

Diethyl *N,N′*-bis(2-hydroxybenzyl)ethylenediamine-*N,N′*-diacetate (2b): colorless needles from hot ethanol (3.51 g, 79%); mp 77−78 °C; TLC R_f = 0.40 (ethyl acetate/hexanes 1:2); HPLC t_R = 10.79 min; ^{1}H NMR (300 MHz, $CDCl_3$) δ 1.28 (t, 6H, *J* = 7.14, OCH_2**CH_3**), 2.73 (s, 4H, N-C**H$_2$**-C**H$_2$**-N), 3.28 (s, 4H, N-C**H$_2$**-CO_2Et), 3.75 (s, 4H, N-**CH$_2$**-Ar), 4.19 (q, 4H, O**CH$_2$**CH_3), 6.77 ('dt', 2H, *J* = 1.16, 7.36, Ar**H**), 6.85 ('dd', 2H, *J* = 1.01, 8.06, Ar**H**), 6.91 ('dd', 2H, *J* = 1.65, 7.51, Ar**H**), 7.19 ('dt', 2H, *J* = 1.71, 7.97, Ar**H**), 9.54 (br s, 2H, ArO**H**). Anal. ($C_{24}H_{32}N_2O_6$ [444.53]) C, H, N.

General Procedure for Partial Hydrolysis of HBED Diesters 2. To a solution of the HBED diester (10 mmol) in the corresponding alcohol (100 mL) was added 2 M NaOH (5 mL, 10 mmol). The clear solution obtained was stirred at 40 °C for 18 h. During this time the sodium salt of the HBED monoester precipitated in the form of very fine colorless crystals. The reaction flask was placed in an ice bath and stirred for further 4 h at 0 °C. The crystals formed were filtered off, washed with ice-cold alcohol (3 × 50 mL), and dried in a high vacuum at 50 °C for 24 h.

Sodium *N,N′*-bis(2-hydroxybenzyl)ethylenediamine-*N*-methoxycarbonylmethyl-*N′*-acetate (3a): colorless microcrystalline powder (2.16 g, 51%); mp 211−213 °C dec; TLC R_f = 0.18 (DCM/MeOH/H_2O/AcOH 90:10:1:0.5); HPLC t_R = 9.17 min; MS (+FAB) *m/z* 425 (MH^+); ^{1}H NMR (300 MHz, DMSO-d_6) δ 2.37 (t, 2H, *J* = 5.6, NC**H$_2$**CH_2N), 2.52 (t, 2H, *J* = 5.6, NCH_2C**H$_2$**N), 2.82 (s, 2H, NC**H$_2$**CO_2H), 3.36 (s, 2H, N-C**H$_2$**CO_2Me) 3.38 (s, 2H, N-C**H$_2$**Ar) 3.44 (s, 2H, N-C**H$_2$**Ar), 3.58 (s, 3H, OMe), 6.60−6.75 (m, 5H, Ar**H**), 6.92 ('dd', 1H, *J* = 1.1, 7.5, Ar**H**), 7.07 ('dq', 2H, *J* = 1.5, 7.7, Ar**H**), 11.20 (br s, 2H, ArO**H**). Anal. ($C_{21}H_{25}N_2NaO_6$ [424.43]) C, H, N, Na^+.

Sodium *N,N′*-bis(2-hydroxybenzyl)ethylenediamine-*N*-ethoxycarbonylmethyl-*N′*-acetate (3b): colorless microcrystalline powder (3.77 g, 86%): mp 192−193 °C dec; TLC R_f = 0.21 (DCM/MeOH/H_2O/AcOH 90:10:1:0.5); HPLC t_R = 9.50 min; MS (+FAB) *m/z* 439 (MH^+); ^{1}H NMR (300 MHz, DMSO-d_6) δ 1.17 (t, 3H, *J* = 7.20, OCH_2C**H$_3$**), 2.37 (t, 2H, *J* = 6.4, NC**H$_2$**CH_2N), 2.51 (t, 2H, *J* = 6.4, NCH_2C**H$_2$**N), 2.79 (s, 2H, NC**H$_2$**CO_2H), 3.33 (s, 2H, N-C**H$_2$**CO_2Et) 3.36 (s, 2H, N-C**H$_2$**-Ar) 3.45 (s, 2H, N-C**H$_2$**Ar), 4.06 (q, 2H, OC**H$_2$**CH_3), 6.58−6.76 (m, 5H, Ar**H**), 6.90 ('dd', 1H, *J* = 1.0, 7.2, Ar**H**), 7.05 ('dq', 2H, *J* = 1.4, 7.4, Ar**H**), 11.25 (br s, 2H, ArO**H**). Anal. ($C_{22}H_{27}N_2NaO_6$ [438.46]) C, H, N, Na.

Sodium[[*N,N′*-bis(2-hydroxybenzyl)ethylenediamine-*N,N′*-diacetato](3−)-*N,N′,O,O′,ON,ON′*]-ferrate(1−), Na-[Fe(hbed)] (4). To a solution of iron(III) chloride hexahydrate (5.41 g, 20 mmol) in 2 M hydrochloric acid (250 mL, 0.5 mol) was added HBED hydrochloride dihydrate (**1**; 9.22 g, 20 mmol). The suspension was stirred at 30 °C until all material went in to solution. Then 4 M sodium hydroxide (150 mL, 0.6 mol) was added with vigorous stirring and cooling in an ice bath. After 1 h at 0 °C the precipitated product was filtered off, washed with ice water (250 mL) and ice-cold methanol (approximately 400 mL) until the filtrate became almost colorless. Drying in a stream of air gave a reddish brown powder (7.22 g, 59%): mp > 300 °C; TLC R_f = 0.29 (DCM/MeOH/H_2O/AcOH 75:27:5:0.5), reddish spot; HPLC t_R = 5.92 min (very broad peak); MS (−ESI) *m/z* 440 ([^{56}Fe(HBED)]$^-$); ^{1}H NMR (300 MHz, DMSO-d_6) no signals, material is paramagnetic. Anal. ($C_{20}H_{20}FeN_2NaO_6$·2NaCl·2H_2O [616.15]) C, H, N, Fe, Na, H_2O.

[[*N,N′*-Bis(2-hydroxybenzyl)ethylenediamine-*N*-methoxycarbonylmethyl-*N′*-acetato](3−)-*N,N′,O,O′,ON,ON′*]-ferrate(0), [Fe(me-hbed)] (5). To an ice-cold suspension of **3b** (877 mg, 2 mmol) in ethanol (100 mL) was added a solution of iron(III) chloride hexahydrate (595 mg, 2.2 mmol) in ethanol (50 mL). After completion of the addition the now deeply purple colored solution was stirred for 30 min at 0 °C. By addition of 1 M NaOH the solution was adjusted to pH 3 and was stirred for a further 2 h at room temperature. The solvent was distilled off in a vacuum at room temperature. The black partly crystalline residue was taken up in dichloromethane, washed (1× buffer pH 7, 2× H_2O, 1× brine), and dried (Na_2SO_4). Precipitation of the iron complex by addition of dry ether gave black fine crystals (600 mg, 64%): mp > 300 °C; TLC R_f = 0.20 (DCM/MeOH/H_2O/AcOH 90:10:1:0.5), purple spot; HPLC t_R = 9.78 min (complex partly dissociates: 25% free ligand detectable); MS (+ESI) *m/z* 470 ([^{56}FeH(me-HBED)]$^+$); ^{1}H NMR (300 MHz, $CDCl_3$) no signals, material is paramagnetic. Anal. ($C_{22}H_{25}FeN_2O_6$ [469.30]) C, H, N, Fe.

Ionization Constants. Potentiometric titrations were performed in 0.15 M KCl at 25 °C with a PCA 101 automatic titrator and the data analyzed with pKaLOGP for Windows software 4.02 (Sirius Analytical Instruments, Forest Row, U.K.). Spectrophotometric titrations were performed with a Beckman DU-7400 diode array spectrophotometer. Before each titration the pH electrode was first calibrated using a pH 7.00 phosphate buffer. Since all constants given in this report are true thermodynamic constants, an additional step was used to convert the operational pH scale (obtained from the mV readings) to a concentration scale where $p_cH = -\log [H^+]$. Before each set of titrations, a blank titration was performed and the pH electrode was standardized using a nonlinear procedure based on the following semiempirical equation:[19]

$$pH = \alpha + Sp_cH + j_H[H^+] + j_{OH}K_w/[H^+]$$

where K_w is the ionization constant for water, *S* is the Nernst slope, j_H and j_{OH} are the asymmetry potentials (or junction potentials) in the acid and alkaline directions, and α is a constant. When a cosolvent was used, the pH electrode was

standardized using the same procedure in the presence of a defined amount of cosolvent and the corresponding K_w value was taken from the literature. Argon was used to prevent carbon dioxide uptake.

Partition Coefficients. Partition coefficients of the free ligands were measured with the pH metric technique[20,21] which basically consists of two linked titrations: a normal titration followed by a two-phase titration in the presence of the partition solvent.

The lipophilicity of the iron chelates was determined by measuring their distribution coefficient at pH 7.40 in (50 mM HEPES, 100 mM NaCl/*n*-octanol) using the shake-flask method.

Conformational Analyses. The conformational analysis studies were performed using the Monte Carlo module of the modeling package Macromodel[22] version 4.0. Water and chloroform solutions were simulated according to the method by Hasel and Still.[23,24] The conformations were generated by random variations of all rotatable bonds in the different molecules, followed by energy minimization with the AMBER[25] force field. The protonation patterns were assigned based on our analysis of the titration curves recorded in media with different dielectric constants. All conformations within 4 kcal/mol of the respective computed global minima were analyzed within the module "Analysis" of the package InsightII[26] (software to convert Macromodel multiconformational files to MSI's archive files by V.T., unpublished results). The analysis was focused on a visual assessment of the shapes of the different molecules and their H-bond patterns, as well as on the graphic plots of the distances between the centroids of the two phenoxy rings. Solvent-accessible surfaces and molecular volumes were computed using the method by Huron and Claverie.[27] The representative conformations chosen for display in the figures of the present work are within 1 kcal/mol of the respective computed global minima.

Iron-Binding Stoichiometry and Complex Stability. The iron-binding stoichiometry was determined at pH 7.40 using the mole ratio variation method also known as the Job plot.[28] The affinity of **3b** (me-HBED) for ferric iron was determined by spectrophotometric titration in 0.15 M KCl. Computation procedures were done as described by Nagano and Metzler[29] using Excel solver.

Kinetic Analyses. The conversion of **5** into **4** was followed spectrophotometrically following extraction with dichloromethane. The organic phase contains me-HBED−Fe while HBED−Fe stays in the aqueous phase. Kinetic analyses were performed by nonlinear regression analysis with Enzfitter (Biosoft, Cambridge, U.K.).

In Vivo Efficacy. The in vivo efficacy of the test compounds was determined in primates using the marmoset (*C. jacchus*) with an adaptation of the *Cebus apella* model of Bergeron et al.[30] Briefly, marmosets were iron-overloaded by injections of iron dextran. For iron-balance studies, animals were kept in metabolic cages an maintained on low-iron diet in order to reduce fecal background. After compound administration the excretion of iron in urine and feces was followed for 2 days. Urinary iron was measured colorimetrically (bathophenantroline method) and fecal iron was determined by atomic aborption spectroscopy.

Supporting Information Available: Figures showing the spectrophotometric titration of me-HBED and kinetics of conversion of **5** into **4** at pH 7.4 and table showing the solvent-accessible surface area in water of compounds **1**, **3a**, **3b,** and **2a**. This material is available free of charge via the Internet at http://pubs.acs.org.

References

(1) Porter, J. B.; Huhens, E. R.; Hider, R. C. The development of iron chelating drugs. *Clin. Hematol.* **1989**, *2*, 257−292.

(2) Hershko, C.; Link, G.; Tzahor, M.; Pinson, A. In *The Development of Iron Chelators for Clinical Use*; Bergeron, R. J., Brittenham, G. M., Eds.; CRC Press: Boca Raton, Ann Arbor, London, Tokyo, 1994; 75pp.

(3) Olivieri, N. F.; Brittenham, G. Iron-chelating therapy and the treatment of thalassemia. *Blood* **1997**, *89*(3), 739−761.

(4) L'Eplattenier, F.; Murase, I.; Martell, A. E. New multidentate ligands. IV. Chelating tendencies of N, N′-di(2-hydroxybenzyl)-ethylenediamine-N,N′-diacetic acid. *J. Am. Chem. Soc.* **1967**, *89*, 837−843.

(5) Grady, R. W.; Hersko, C. HBED: a potential oral iron chelator. *Ann. N. Y. Acad. Sci.* **1990**, *612*, 361−368.

(6) Peter, H. H.; Bergeron, R. J.; Streiff, R. R.; Wiegand, J. A comparative evaluation of iron chelators in a primate model. In *The Development of Iron Chelators for Clinical Use;* Bergeron, R. J., Brittenham, G. M., Eds.; CRC Press Inc.: Boca Raton, 1993; pp 373−394.

(7) Grady, R. W.; Salbe, A. D.; Hilgartner, M. W.; Giardina, P. J. Preliminary results from a phase I clinical trial of HBED. In *The Development of Iron Chelators for Clinical Use;* Bergeron, R. J., Brittenham, G. M., Eds.; CRC Press Inc.: Boca Raton, 1993; pp 395−406.

(8) Grady, R. W.; Salbe, A. D.; Hilgartner, M. W.; Giardina, P. J. Results from phase I clinical trial of HBED. *Adv. Exp. Med. Biol.* **1994**, *356*, 351−359.

(9) Pitt, C. G.; Bao, Y.; Thompson, J.; Wani, M. C.; Rosenkrantz, H.; Metterville, J. Esters and Lactones of Phenolic Amino Carboxylic Acids: Prodrugs for Iron Chelation. *J. Med. Chem.* **1986**, *29*, 1231−1237.

(10) Yasuda, M. Dissociation constants of some carboxylic acids in mixed aqueous solvents. *Bull. Chem. Soc. Jpn.* **1959**, *32*, 429−432.

(11) Shedlovsky, T.; Kay, R. L. The ionization constant of acetic acid in water-methanol mixtures at 25 °C from conductance measurements. *J. Am. Chem. Soc.* **1956**, *60*, 151−155.

(12) Wakita, K.; Yoshimoto, M.; Miyamato, H.; Watanabe, H. A method for the calculation of the aqueous solubility of organic compounds by using new fragment solubility constants. *Chem. Pharm. Bull.* **1986**, *34*, 4663.

(13) Pagliara, A.; Carrupt, P.-A.; Caron, G.; Gaillard, P.; Testa, B. Lipophilicity Profiles of Ampholytes. *Chem. Rev.* **1997**, *97*, 3385−3400.

(14) Von Geldern, T. W.; Hoffman, D. J.; Kester, J. A.; Nellans, H. N.; Dayton, B. D.; Calzadilla, S. V.; Marsh, K. C.; Hernandez, L.; Chiou, W.; Dixon, D. B.; Wu-Wong, J. R.; Opgenorth, T. J. Azole endothelin antagonists. 3. Using ΔlogP as a tool to improve absorption. *J. Med. Chem.* **1996**, *39*, 982−991.

(15) Young, R. C.; Mitchell, R. C.; Brown, T. H.; Ganellin, C. R.; Griffiths, R.; Jones, M.; Rana, K. K.; Saunders, D.; Smith, I. R.; Sore, N. E. Development of a new physicochemical model for brain penetration and its application to the design of centrally acting H2 receptor histamine antagonists. *J. Med. Chem.* **1988**, *31*, 657−671.

(16) Steyaert, G.; Lisa, G.; Gaillard, P.; Boss, G.; Reymond, F.; Girault, H. H.; Carrupt, P.-A.; Testa, B. Intermolecular forces expressed in 1,2-dichloroethane-water partition coefficients. *J. Chem. Soc., Faraday Trans.* **1997**, *93*(3), 401−406.

(17) Amidon, G. L.; Lennernas, H.; Shah, V. P.; Crison, J. R. A theoretical basis for a biopharmaceutic drug classification: the correlation of in vitro drug product dissolution and in vivo bioavailability. *Pharm. Res.* **1995**, *12*, 413−420.

(18) Still, W. C.; Kahn, M.; Mitra, A. *J. Org. Chem.* **1978**, *43*, 2923.

(19) Avdeef, A. Weighting scheme for regression analysis using pH data from acid−base titration. *Anal. Chim. Acta* **1983**, *148*, 237−244.

(20) Clarke, F. H.; Cahoon, N. M. Ionization constants by curve fitting: determination of partition and distribution coefficients of acids and bases and their ions. *J. Pharm. Sci.* **1987**, *76*, 611−620.

(21) Avdeef, A.; Comer, J. E. A.; Thomson, S. J. pH-metric logP. 3. Glass electrode calibration in methanol−water, applied to pK_a determination of water insoluble substances. *Anal. Chem.* **1993**, *65*, 42−49.

(22) Mohamadi, F.; Richards, N. G. J.; Guida W. C.; Liskamp, R.; Lipton, M.; Caufield, C.; Chang, G.; Hendrickson, T.; Still, W. C. MacroModel An Integrated Software System for Modeling Organic and Bioorganic Molecules using Molecular Mechanics. *J. Comput. Chem.* **1990**, *11*, 440−467.

(23) Hasel, W.; Hendrickson, T.; Still, W. C. A Rapid Approximation to the Solvent Accessible Surface Areas of Atoms. *Tetrahedron Comp. Methodol.* **1988**, *1*, 103−116.

(24) Still, W. C.; Tempczyk, A.; Hawley, R. C.; Hendrickson, T. Semianalytical Treatment of Solvation for Molecular Mechanics and Dynamics. *J. Am. Chem. Soc.* **1990**, *112*, 6127−6129.

(25) Weiner, S. J.; Kollman, P. A.; Nguyen, D. T.; Case, D. A. An All Atom Force Field for Simulations of Proteins and Nucleic Acids. *J. Comput. Chem.* **1986**, *7*, 230−252.

(26) MSI. *InsightII Molecular Modeling System* (v. 95.0); MSI: San Diego, CA, 1995.

(27) Huron, M.; Claverie, P. Calculation of Molecular Surfaces and Volumes. *J. Phys. Chem.* **1972**, *76*, 2123−2133.

(28) Huang, C. Y. Determination of binding stoichiometry by the continuous variation method: the Job plot. *Methods Enzymol. 87*, 509−525.
(29) Nagano, K.; Metzler, D. E. Machine computation of equilibrium constants and plotting of spectra of individual ionic species in the pyridoxal-alanine system. *J. Am. Chem. Soc.* **1967**, *89*, 2891, 2900.
(30) Bergeron, R. J.; Streiff, R. R.; Weigand, J.; Vinson, J. R. T.; Luchetta, G.; Evans, K. M.; Peter, H. H.; Jenny, H. B. A. Comparative Evaluation of Iron Clearance Models. *Ann. N. Y. Acad. Sci.* **1990**, *612*, 378−393.

JM990261N